Title

Unravelling the neural dynamics of hypnotic susceptibility: Aperiodic neural activity as a central feature of hypnosis

Authors

Mathieu Landry[1], Jason da Silva Castanheira[2], Jérôme Sackur[3], Amir Raz[4], David Ogez[5], Pierre Rainville[6,7], Karim Jerbi[1,7,8,9]

Affiliations

[1] Département de psychologie, Université de Montréal, Montreal, Qc, Canada

[2] NEURO, McGill University, Montreal, Qc, Canada

[3]Laboratoire de Sciences Cognitives et Psycholinguistique, ENS, PSL University, EHESS, CNRS, Paris, France

[4]Institute for Interdisciplinary Behavioral and Brain Sciences, Chapman University, Irvine, CA, USA. 92618.

[5]Maisonneuve-Rosemont Hospital, Montreal, Qc, Canada

[6]Départment de stomatologie, Faculté de médecine dentaire,Université de Montréal, Montréal, Canada

[7]Centre de recherche de l'Institut universitaire de gériatrie de Montréal (CRIUGM), Université de Montréal, Montréal, Canada

[8]MILA - Quebec Artificial Intelligence Institute, Montreal, Qc, Canada

[9]UNIQUE Center (Quebec Neuro-AI Research Center), Montreal, Qc, Canada

Corresponding author: Mathieu Landry (mathieu.landry2@umontreal.ca)

Abstract: x words
Body: x words

Key Words

Hypnosis, Resting-State EEG, Spectral Analysis, Connectivity, Machine Learning, Classification

Acknowledgments
M.L. acknowledges support from the Fonds de Recherche du Québec – Nature et Technologies, the Natural Science and Engineering Research Council of Canada. M.L., J.S. and A.R. acknowledge support from the Bial Foundation (Grant #280/16). J.d.C. acknowledges support from the Natural Science and Engineering Research Council of Canada. D.O. acknowledges support from the Fonds de Recherche du Québec.

Contributions
M.L., J.d.C. P.R., and K.J. conceptualization. M.L. and J.d.C. implementation and formal data analysis. M.L., J.S., and A.R. funding. All authors wrote the manuscript.

Competing Interests
All authors declare no competing interest.

Data availability
Data for the analyses supporting the current study is publicly available on the Open Science Framework repository:

Code Availability
Code for the analyses supporting the current study is publicly available on the Open Science Framework repository:

Abstract
The ability for hypnotic responding is marked by great inter-individual variation in the population, while the neural underpinning of this variability remains elusive. The current work leveraged multivariate statistics and machine learning to probe the neural dynamics underlying inter-individual differences in hypnotic susceptibility. We assessed the efficacy of linear classifiers in distinguishing between high and low hypnotic susceptible individuals using neural features from resting-state electroencephalography (EEG) both pre- and post-hypnotic induction. Our focus encompassed both aperiodic and periodic components of the power spectrum, and graph theoretical measures derived from functional connectivity patterns. Several neural features from both pre- and post-induction significantly differentiated susceptibility levels, which underscores the complex dynamics of hypnotic phenomena. Based on model comparisons and feature ranking, we discerned the pre-induction aperiodic exponent as the primary discriminating neural feature, while periodic activity did not differ between groups. This novel finding not only resonates with the increasing emphasis on this neural component in broader EEG research but also promotes the idea that the primary neural distinction in hypnotic susceptibility is evident at baseline, even before hypnosis. Based on prevailing interpretation of aperiodicity in the EEG signal, our findings support the idea that hypnotic susceptibility might be an inherent trait reflected in the balance of cortical excitation and inhibition.

Significance Statement

Hypnotic phenomena reflect the ability to alter one's subjective experiences based on targeted verbal suggestions. While research has made strides in understanding the cognitive aspects underlying the variability in one's susceptibility to hypnosis, the brain correlates remain largely elusive. Addressing this gap, our study employs multivariate pattern classification and machine learning to predict hypnotic susceptibility. By recording electroencephalography (EEG) before and after hypnotic induction and analyzing diverse neurophysiological features, we identify several features that differentiate between high and low hypnotic susceptible individuals for both pre- and post-induction periods, which underscores the multifaceted nature of hypnotic phenomena. Our analysis revealed that the paramount discriminative feature is arrhythmic (i.e., non-oscillatory) EEG activity prior to the induction—a novel discovery in the field. This finding, that the chief EEG marker is observed even before hypnosis, aligns with the idea that hypnotic susceptibility represents an inherent trait reflecting the balance between excitation and inhibition in neural activity.

Introduction

Hypnotic phenomena reflect responding to hypnotic suggestions in a manner that alters perception, cognition, ideomotor actions, and emotional states via top-down mental processes (Lynn et al., 2019; Terhune et al., 2017). This response is often characterized by changes in phenomenology, including sensations of profound relaxation, heightened mental absorption, shifts in volitional control and automaticity, vivid imaginative experiences, and even temporal distortions (Cardeña, 2016; Lifshitz et al., 2019; Pekala, 2015; Rainville & Price, 2003; Timmermann et al., 2023). These variations in phenomenology are often construed as a defining feature of hypnotic phenomena (Dienes & Perner, 2007; Weitzenhoffer, 1980). In this way, hypnosis encompasses the directed modulation of information processing in a manner that aligns with the content of hypnotic suggestions (e.g., altering the neural representation and interpretation of nociceptive signals in the context hypnotic analgesia; Rainville et al., 1997), and the spontaneous alterations across diverse phenomenological dimensions (e.g., Cardeña, 2005). Hypnotic phenomena are therefore multifaceted and hardly reducible to a single dimension or feature.

The neuroscientific landscape of hypnosis is marked by intricate complexity, characterized by several hypotheses, methodologies, and interpretive frameworks (Elkins, 2016; Nash & Barnier, 2008). This heterogeneity includes studies investigating the neurophenomenological facets of hypnosis (e.g., Rainville et al., 2019), alongside endeavors aiming to uncover the neural underpinnings of hypnotic responsiveness (e.g., Desmarteaux et al., 2021). The primary consequence of this heterogeneity is that the resulting body of research exhibits a wide diversity of findings (Landry et al., 2017; Vanhaudenhuyse et al., 2014). Within the experimental context of electrophysiological recordings, research shows that multiple aspects of the signal relate to hypnotic phenomena. These findings encompass modulations of spectral power (e.g., De Pascalis, 1993), evoked responses (e.g., Spiegel et al., 1985), the fractal component of the electroencephalographic signal (Lee et al., 2007), shifts in connectivity patterns (e.g., Jamieson & Burgess, 2014), as well as changes in the intricate organization of network topology (Panda et al., 2023). Likewise, neuroimaging studies link hypnotic phenomena to diverse brain regions, including alterations in the interplay among resting-state networks—such as the central executive, the salience, and the default networks (Deeley et al., 2012; Demertzi et al., 2011; Jiang et al., 2016; McGeown et al., 2009). This wide variety of findings in the literature reflects the inherent complexity of hypnosis and demonstrates the multi-faceted nature of hypnotic responding (Barnier et al., 2022; Woody et al., 2005). In sum, neuroscience research underscores that hypnotic responsiveness involves several components (Landry & Rainville, in press).

To tackle the inherent complexity of hypnotic phenomena at the brain level, neuroscientific research largely centers on the exploration of three pivotal variables: Susceptibility to hypnotic suggestions, the induction procedure, and the impact of suggestions (Landry & Raz, 2015; Mazzoni et al., 2013). Susceptibility to hypnotic suggestions refers to a stable psychological trait that primarily signifies the ability to effectively respond to direct verbal suggestions within controlled and standardized settings (Laurence et al., 2008; Woody & Barnier, 2008). Notably, susceptibility to

hypnotic suggestions serves as a predictive indicator across both experimental and clinical contexts of hypnosis (Barnier et al., 2014; Montgomery et al., 2011). The induction procedure constitutes an integral part of most hypnotic protocols (Yapko, 2015). During this phase, the operator, referred as the "hypnotizer," imparts a sequence of instructions to individuals undergoing hypnosis with the aim of enhancing their readiness to respond to subsequent suggestions(Terhune & Cardeña, 2016). This process frequently involves dispensing information and guidance designed to elevate preparedness and receptiveness, achieved through procedural identification, heightened relaxation, and intensified mental absorption. The induction procedure has also been linked to spontaneous shifts in phenomenology among highly hypnotically susceptible individuals (Cardeña, 2014; Pekala & Kumar, 2007; Vanhaudenhuyse et al., 2019), as well as discernible alterations in neural activity (Panda et al., 2023; Rainville et al., 1999). Lastly, suggestions emerge as cognitive constructs, often conveyed through the medium of imagery and metaphors via verbal instructions, with the aim of eliciting specific experiences and modifying mental processes within hypnotized individuals through top-down regulation (Braffman & Kirsch, 1999; Kirsch & Braffman, 2001; Terhune et al., 2017). Suggestions will invite individuals undergoing hypnosis to engage into counterfactual experiences. Collectively, these variables contribute significantly to the variance underpinning the manifestation of hypnotic phenomena at the neural level.

The primary objective of the current study is to elucidate the underlying neural dynamics associated with hypnotic susceptibility and the induction procedure. This is accomplished through the integration of high density resting-state electroencephalography (rs-EEG), advanced multivariate pattern classification techniques, and machine learning methodologies. Our work builds upon previous EEG-based research of hypnosis that has revealed distinct modulations in the power spectrum (e.g., De Pascalis, 1993) and intricate network topologies under the purview of graph theory (Panda et al., 2023). In this regard, previous research highlights the contribution of multiple broad bands of the EEG signal (e.g., theta band activity; Sabourin et al., 1990). We accordingly aim to assess the discriminative capabilities of a linear classifier in accurately categorizing individuals with high hypnotic susceptibility (HHSIs) and low hypnotic susceptibility (LHSIs) both before the hypnotic induction and based on the effect of the induction where we evaluated the effects of the induction procedure by subtracting pre-induction from the post-induction values (post- minus pre-induction: Δ induction; **Figure 1**). Our approach therefore examines both the pre-induction period and the effect of the induction procedure. We hypothesize that numerous neural attributes inherent to rs-EEG exhibit direct relevance to our focal variables. Following previous work, we examined neural features relative to spectral power and network topologies derived from connectivity patterns. Our approach was twofold. First, we tested each neural feature separately. Next, we identified the most discriminant one using model comparisons, where we evaluated all combinations of relevant features, and feature ranking when all relevant features are included in the model. In this way, we were able to ascertain which EEG patterns best characterize hypnotic susceptibility.

Electrophysiological signal power spectra encompass both aperiodic and periodic components (Buzsáki & Draguhn, 2004; Miller et al., 2009). The aperiodic component

corresponds to scale-free arrhythmic activity pattern, marked by a spectral density that approximates a power-law distribution ($P \propto 1/f^{\beta}$) within the frequency domain. Conversely, the periodic component denotes rhythmic activity that manifest as discernible peaks in the frequency domain. This component corresponds to oscillatory neural patterns along the time series. Recent investigations underscore the importance of concurrently considering both components when exploring electrophysiological signals within the frequency domain, particularly for the purpose of identifying oscillatory neural activity (Donoghue et al., 2022; Wilson et al., 2022).

Recent work demonstrates that the aperiodic and periodic components of the EEG can be effectively parameterized in logarithmically transformed power and frequencies domains, wherein the aperiodic component is estimated using a linear model, while the peaks of the periodic component is estimated through Gaussian functions (Donoghue et al., 2020). The aperiodic component's linear model entails parameters encompassing both the slope and the offset, and periodicity rests on parameters that estimates the center frequency, width, and relative amplitude of the peaks of the spectral distribution. Both the aperiodic and periodic elements of the power spectrum hold relevance across a wide range of psychological phenomena, spanning sensations and cognition, developmental trajectories and aging, as well as clinical and pharmacologically-induced mental states, and altered states of consciousness (Gerster et al., 2022; He, 2014; Lopes da Silva, 2013; Maschke et al., 2023). We relied on this parameterization technique to assess periodic and aperiodic dimensions of the rs-EEG signal.

Graph theoretical analyses are designed to extract meaningful information about the structural and functional architecture of complex networks (Bullmore & Sporns, 2009). Applying this analytical framework to neural connectivity patterns has yielded a large body of findings relating features of brain networks to various aspects of the mind (Farahani et al., 2019). Specifically, dynamical reconfigurations of network structures relative environmental demands is viewed as a one of the brain's features that enable flexible cognitive abilities (Cole et al., 2014). Evidence indicates that this is done by balancing integration and segregation of information across brain networks (Cohen & D'Esposito, 2016; Wang et al., 2021). Graph theoretical metrics are designed to estimate these aspects of brain networks. In context of hypnosis, a recent EEG study employed graph theory to show that the hypnotic induction increases brain networks in HHSIs segregation in delta and alpha bands, and integration in the beta-band (Panda et al., 2023). Accordingly, the hypnotic procedure reconfigures functional brain networks both at local and global levels. The present work therefore focused on these topological aspects of rs-EEG.

Methods

Participants. Our recruitment procedure comprised two stages. First, potential participants were invited to a pre-screening session, during which we assessed their hypnotic susceptibility using the Harvard Group Scale of Hypnotic Susceptibility, Form A (HGSHS:A; Shor & Orne, 1962). Subsequently, we selected 75 individuals from this initial pool to undergo EEG recordings. For the present study, we focused on neural activity data from 40 individuals (27 females, mean age of 21.98 y.o. (st.dev. = 4.41)) based on

their HGSHS:A scores. Specifically, we included individuals who scored above 8, indicating high hypnotic susceptibility (HHSIs), and individuals who scored below 4, indicating low hypnotic susceptibility (LHSIs). This work aligns with previous studies focusing on high and low hypnotic susceptible individuals to maximize the detection of the effect. We Participants were not informed of their scores. Participants who completed the second part of our recruitment procedure received monetary compensation. All study procedures were approved by the local institutional review board. Participants provided written consent.

Our sample size was determined based on prior research investigating the impact of hypnotic susceptibility on spectral features and connectivity measures during rs-EEG, which reported statistically significant findings. One recent study examined differential entropy and connectivity patterns in the theta, alpha, and beta frequency ranges across the entire scalp, comparing individuals with high and low hypnotic susceptibility (Keshmiri et al., 2020). The results indicated effect sizes ranging from dz = 1.92 to dz = 0.46 at parietal and occipital sites, which entails that a total sample size ranging from 5 to 55 participants would be necessary to achieve a power level of 0.8 at an alpha level of 0.05. However, not all studies consistently demonstrate an effect of hypnotic susceptibility on spectral power. One study reported no significant differences in spectral power between high (N=12) and low (N=11) hypnotic susceptibility individuals across multiple channels based on a multivariate approach (Jamieson & Burgess, 2014). In turn, this assay found a significant interaction between hypnotic induction and susceptibility in the theta and beta frequency ranges based on connectivity patterns at the scalp level. Similarly, another study reported a significant difference in frontoparietal connectivity for alpha oscillations between high (N=28) and low (N=19) hypnotic susceptibility groups (Terhune et al., 2011). Our sample size was therefore adequate to detect the effects of hypnotic susceptibility and hypnotic induction on power spectra and network topologies.

Procedure. The assessment of hypnotic susceptibility was conducted following the standard procedure of the HGSHS:A in a separate experimental session on a different day. The experimental procedure consisted of a 5-minute rs-EEG that was recorded at baseline (i.e., pre-induction period), followed by the hypnotic induction procedure, and subsequently, another 5-minute rs-EEG recording.

During the EEG recording, participants were seated in a quiet and dimly lit room. The experimenter, who conducted the induction procedure, positioned themselves approximately one meter behind the participants throughout the experiment. We recorded the baseline EEG for all participants before the induction-related rs-EEG, instead of counterbalancing our experimental conditions. This approach prevented contamination (i.e., carry-over effects) of the baseline period by the hypnotic induction, as it is challenging to determine the duration required for the effects of hypnosis to wash out after the de-induction. Additionally, since the objective of the current study was to differentiate highly hypnotic susceptible individuals from those with low susceptibility, the order of the baseline and induction-related EEG recordings was deemed irrelevant.

During the baseline recording, participants were instructed by the experimenter to close their eyes while remaining vigilant. For the induction period, the experimenter read a script (see supplementary material), which included instructions for participants to close their eyes, and the 5-minute rs-EEG recording was conducted after the completion of the induction.

Electroencephalography. We recorded EEG signals using 64 Ag/AgCl active electrodes at a sampling rate of 1000 Hz (ActiCap System; Brain Products GmbH; Gilching, Germany). We positioned additional bipolar electrodes at the outer canthi, as well as the superior and inferior orbits of the left eye. We kept impedances of all electrodes below 10 kΩ, while all electrophysiological signals were amplified (ActiChamp System; Brain Products GmbH; Gilching, Germany). Electrode impedances were kept below 10 k∧. Data was collected online at 1000Hz and down sampled to 250Hz offline for data analysis. Data acquisition was done via Brain Recorder (Brain Products Inc., GmbH) while pre-processing and data analysis were completed through Brain Vision Analyzer, Brainstorm (Tadel et al., 2011), and custom MATLAB scripts (version R2022A; MathWorks Inc, MA). Bad electrodes were topographically interpolated using spherical splines (< 3% electrodes). EEG recordings were re-referenced to the average of all EEG electrodes offline. All EEG data were inspected for muscle-related, eye movement or technical artifacts, which were removed before continuing the analysis.

Spectral features. Spectral features were computed individually for each channel using the *specparam* algorithm for spectral parametrization as implemented in Brainstorm (Figure 1A; Donoghue et al., 2020). The *specparam* algorithm decomposes power spectra into periodic and aperiodic (1/f-like) components by fitting the power spectral density in log-log space. The periodic component is characterized by the center frequency, bandwidth, and relative amplitude of the oscillatory peak, while the aperiodic component is defined by the offset and slope of the power spectrum density. In our analysis, we employed the model-selection implementation of specparam to fit the power spectral density from 1 to 40Hz, considering up to 6 peaks, with a minimum peak height of 1db, a peak threshold of 2, a proximity threshold of 0.75, peak width limits between 0.5 to 12 Hz, and a fixed aperiodic mode. Goodness-of-fit was evaluated based on mean-square error, and no significant differences were observed between high and low hypnotic susceptible individuals for the pre-induction period and Δ induction. Specifically, AUC for classification was .51 ($p > .5$) for pre-induction rs-EEG and .49 (for Δinduction on rs-EEG using the multivariate pattern classification described below. We then extracted the power spectrum values for the periodic component of each EEG channel by subtracting the aperiodic component from the power spectrum density. Finally, we calculated the average spectrum values separately for delta (1 to 3.5Hz), theta (4 to 7.5Hz), alpha (8 to 13.5Hz), and beta (14 to 39Hz) broadband frequencies. In summary, our analysis encompassed six spectral features: the offset and slope of the aperiodic component, as well as corrected power for delta, theta, alpha, and beta oscillations.

Features of network topology. To extract network topology features, we utilized graph theory metrics on sensor-level connectivity patterns, employing the Brain Connectivity Toolbox (**Figure 1B**; Rubinov & Sporns, 2010). Initially, we applied the Hilbert

transformation to filter the rs-EEG data at specific frequency bands, namely delta (2 to 4Hz), theta (5 to 7Hz), alpha (8 to 12Hz), beta (15 to 29Hz), and gamma (30 to 50Hz). Subsequently, we estimated functional connectivity between all electrode pairs using the weighted Phase Lag Index (wPLI) to account for volume conduction effects on brain connectivity estimation (Vinck et al., 2011). Then, we opted to normalize the edges into weights ranging from 0 to 1 rather than converting the 64 by 64 functional network into sparse and binarized patterns (Rubinov & Sporns, 2011). This approach ensured the preservation of valuable information without loss due to subjective thresholding choices. From these weighted undirected connectivity matrices, we extracted three distinct graph measures for all frequency bands: The clustering coefficient, derived from the geometric mean of local triangle configurations associated with each node, which provides insight into the extent of node clustering (Onnela et al., 2005); global efficiency, measured as the inverse of the shortest path length, that quantifies the level of shared information across the entire network (Latora & Marchiori, 2001); and global modularity to estimate the degree to which networks are divided into communities (Newman, 2006). These graph theory metrics allowed us to evaluate network integration and segregation as a function of hypnotic induction and susceptibility to hypnotic suggestions. Our graph theoretical approach therefore yielded three separate neural features, clustering coefficient, global efficiency and global modularity across all broad frequency bands.

Multivariate pattern analysis and leave-one-out cross-validation. We employed a multivariate pattern analysis combined with a leave-one-out cross-validation strategy to train and test linear support vector machine (SVM) models. The objective was to discriminate between high and low hypnotic susceptible individuals based on spectral and network topological features (**Figure 1C**). To minimize classification biases, we carefully balanced the classes in our training set, including 16 high and 16 low hypnotic susceptible individuals in each iteration (Thölke et al., 2022). In each iteration of the cross-validation process, one participant was left out for testing the SVM model, while we randomly selected 16 participants from each class for the training set. This procedure was repeated to ensure that each participant served as a test case 10 times for comprehensive cross-validation. The SVM linear model was trained using the 64 EEG channels as features for classification. We assessed the classification performance using the area under the curve (AUC).

The observed classification performance was compared to a surrogate distribution generated from 1000 random permutations. In each permutation, the class labels were randomly shuffled during the training process (Combrisson & Jerbi, 2015). Statistical significance was set at alpha = .05. The observed classification performance was considered statistically significant only if it outperformed 95% the performance of the upper-part (i.e., one-tail) surrogate distribution.

To facilitate interpretation, we further transformed the weights of the SVM classifiers based on the covariance of the training dataset (Haufe et al., 2014). These transformed weights were then averaged across all training iterations. We also extracted PSD and graph theoretical values for the channels where we observed the top 5% SVM

weights to better understand how hypnotic susceptibility and the induction procedure impacted rs-EEG.

We evaluated spectral features and clustering coefficients for pre-induction and Δinduction separately. Note that we also evaluated the post-induction rs-EEG recording alone (available in supplementary material).

In addition to EEG, we applied our multivariate classification approach to vertical and horizontal electro-oculogram signals (VEOG and HEOG) to determine whether we could discriminate between HHSIs and LHSIs across both pre-induction and Δinduction separately. This classification procedure showed that we could not discriminate between HHSIs and LHSIs based on signals from eye movements (see supplementary material).

Logistic regressions for global efficiency and modularity. To assess the predictive power of global efficiency and modularity in relation to hypnotic susceptibility (low versus high), we utilized logistic regression modeling in JASP (Version 0.17.2.1; JASP Team, 2023). Since global efficiency and modularity are network-level metrics, we opted for logistic regression instead of linear SVM classification and cross-validation. To avoid conducting multiple comparisons, we included all features from the frequency bands as predictors in a single regression model:

Logit(Hypnotic Susceptibility) = β0 + β1(G.E delta) + β2(G.E theta) + β3(G.E alpha) + β4(G.E beta)+ β5(G.E gamma) + β6(M. delta) + β7(M. theta) + β8(M. alpha) + β9(M. beta) + β10(M. gamma)

where G.E represents global efficiency, and M. represents modularity across the different frequency bands.

We evaluated the statistical significance of each regression coefficient at the alpha level of .05.

Feature comparisons. The previous analyses allowed us to identify spectral and network features from the pre-induction and Δinduction rs-EEG that differentiate between high and low hypnotic susceptible individuals on their own. Next, we aimed to ascertain the top discriminant feature when we combine them. Our approach was twofold (**Figure 1D**).

First, we relied on model comparisons. Using the previously described multivariate pattern classification analysis and leave-one-out cross-validation approach, we trained and tested SVM models that incorporated all possible combinations of features we previously identified as statistically significant on their own. This assessment was performed three times: once for the pre-induction rs-EEG period, then for Δinduction rs-EEG data, and thirdly for all possible combinations of significant features from both the pre-induction rs-EEG and Δinduction. For each model, we calculated the AUC as a measure of classification performance. To compare the classification performance of all models, we utilized McNemar's test (McNemar, 1947), which is a reliable method for comparing classification performances based on contingency tables (Dietterich, 1998).

To account for multiple comparisons, we corrected the p-values from these tests using the false discovery rate correction method proposed by Benjamini and Hochberg (1995).

Second, we relied on feature ranking. Here included all significant features into SVM models and then ranked the absolute value of the SVM weights following the procedure from Haufe et al. (2014) described earlier. We applied this feature ranking procedure three times: once for all significant features from the pre-induction rs-EEG, second for all significant features for Δinduction, and thirdly for significant features from both the pre-induction and Δinduction rs-EEG.

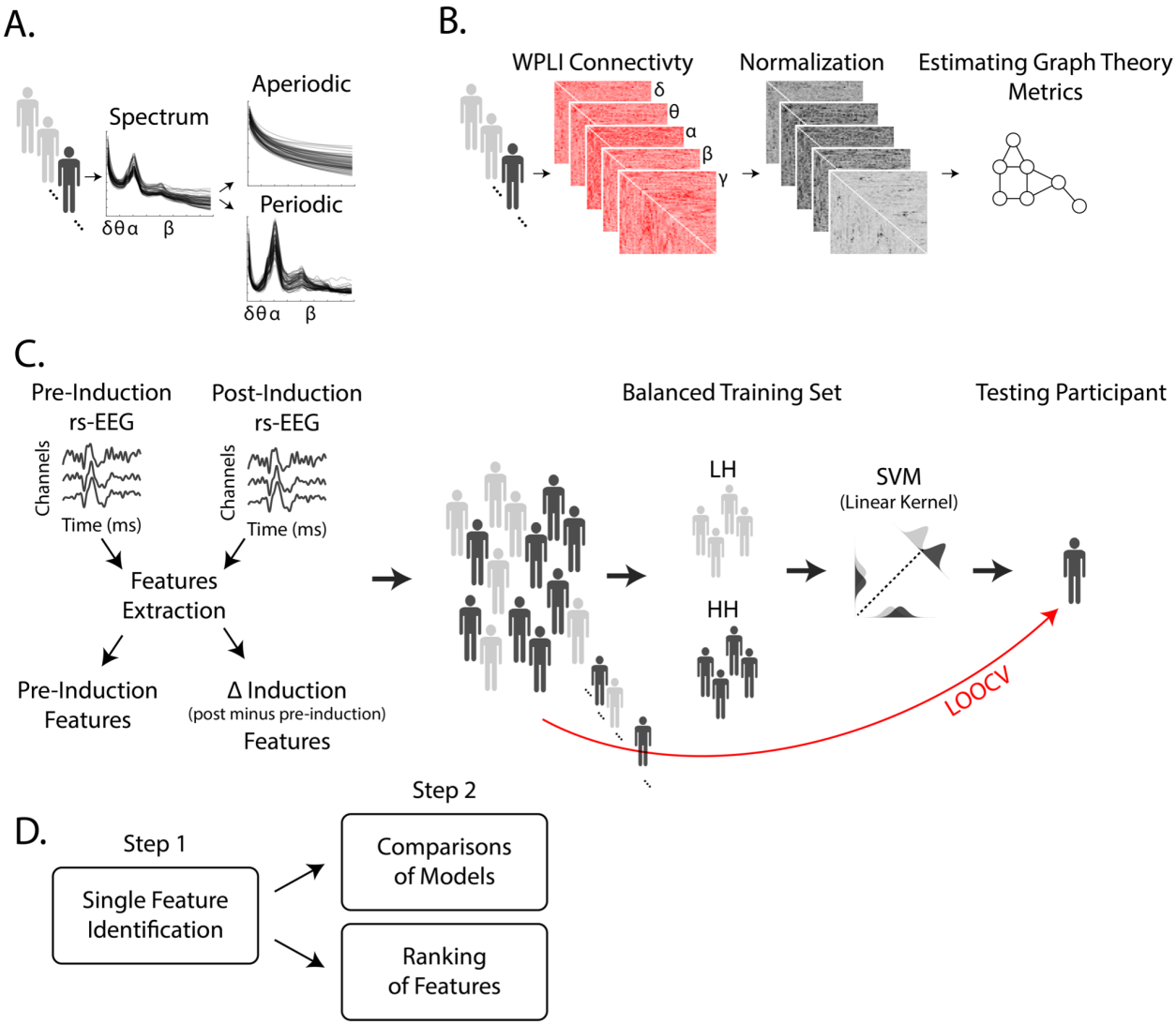

Figure 1. Analysis pipeline for extracting power spectrum and network topology features and performing multivariate pattern analysis with leave-one-out cross-validation. **A.** Aperiodic and periodic components of the power spectrum were estimated for each participant using 5 minutes of eye-closed rs-EEG data, both pre- and Δinduction. **B.** Connectivity patterns between EEG channels were calculated using weighted Phase Lag Index (wPLI) across delta, theta, alpha, beta, and gamma frequencies. The connectivity matrices were normalized from 0 to 1 (Rubinov & Sporns, 2011). Clustering coefficient, global efficiency, and modularity were computed using graph theory for each network. **C.** High and low hypnotic susceptible

individuals were classified based on these metrics using multivariate pattern analysis with leave-one-out cross-validation (LOOCV) employing linear Support Vector Machine (SVM). EEG channels were included as features of this linear model. Each training iteration included balanced classes of low (light grey) and high (dark grey) hypnotic susceptible individuals, while one participant was left out for validation. **D.** We adopted a 2 steps approach to ascertain the top neural feature for discriminating high and low hypnotic susceptible individuals across pre- and Δinduction period. At Step 1, we evaluated all features alone. After identifying features that were relevant for classification. At step 2, we performed comparisons of models comprising all possible combinations of neural features that enabled classification of high and low hypnotic susceptible individuals better than chance-level on their own. We also performed ranking of these neural features.

Results

Spectral features. For the pre-induction period, our SVM classification yielded statistically significant results for the aperiodic exponent (**Figure 2A**; AUC = .69, $p < .001$). However, classification performance based on other spectral features, including oscillatory activity, did not reach significance (**Figure 2A**). We conducted further analysis to examine the weights of the classifiers, which provided insights into the specific contributions of the topographical features (**Figure 2B & 2C).** Notably, we observed a widespread neural pattern indicating that high hypnotic susceptible individuals exhibit a greater slope of the aperiodic component across the entire scalp. However, this pattern was particularly pronounced in the anterior part of the frontal site (**Figure 2B**; with the highest averaged coefficient value observed at channel AF8) and the right temporal region. Lastly, we examined the slope exponent values across pre-induction and Δinduction periods for channels where we observed the top 5% SVM weights during the pre-induction period (AF8, FP1, T8). Here, exponent values were higher for HHSIs compared to LHSIs for the pre-induction periods (**supplementary Figure 1A and 1B**). There was no such difference for Δinduction (**supplementary Figure 1C**). These findings highlight the importance of aperiodic activity relative to hypnotic susceptibility, while the induction procedure does not alter this neural feature.

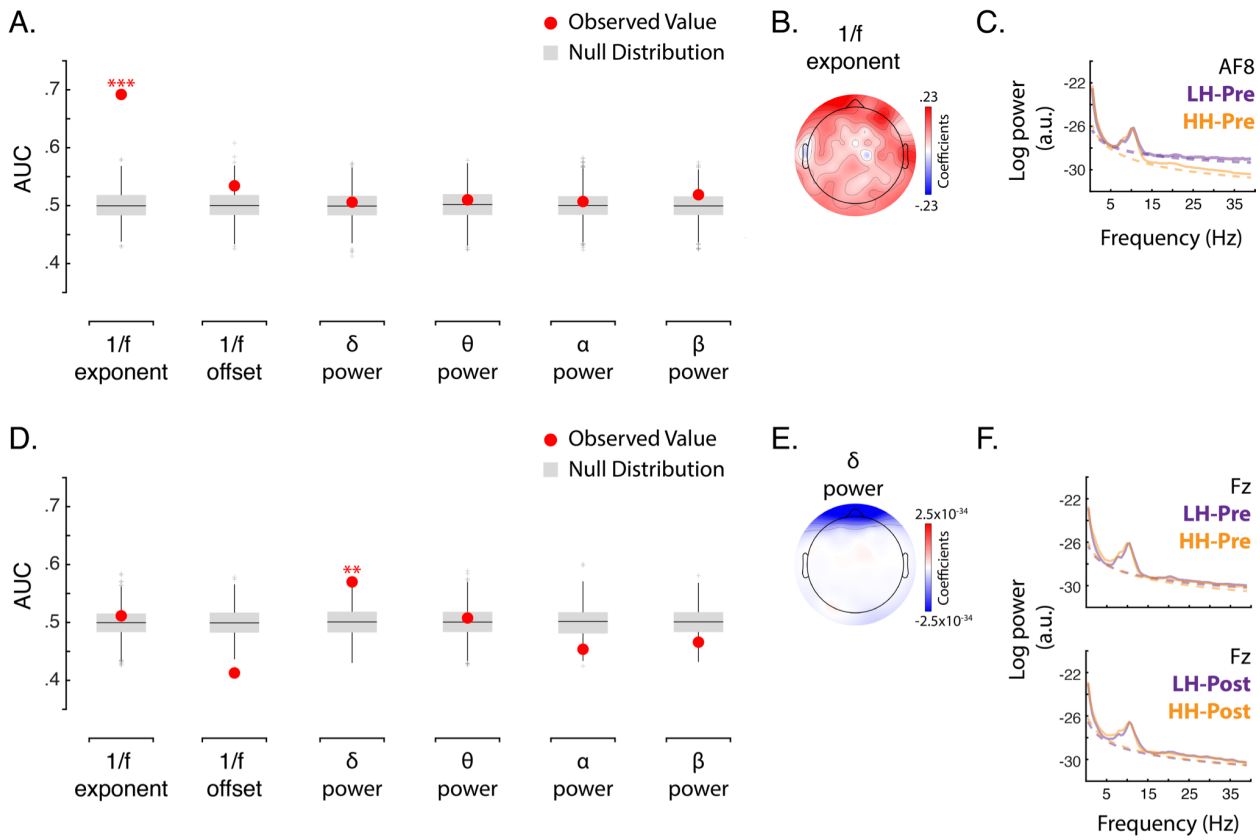

Figure 2. Panels A, B, and C show analysis for pre-induction rs-EEG. Panels D, E, and F show analysis for Δinduction rs-EEG. Panels A and D show AUC values for assessing classification performances of SVM linear models for accurately classifying high and low hypnotic susceptible individuals in LOOVC based on aperiodic and periodic features of the power spectrum during the rs-EEG pre-induction period (A) and the Δ induction period (D). Red dots show observed AUC values. Boxplot shows surrogate null distributions based on random permutations where we shuffled the labels during training. The bottom and top whiskers indicate the first and third quartiles, respectively. Three asterisks indicate statistical significance at $p < .001$, two asterisks at $p < .01$, one asterisk at $p < .05$. B and E show the averaged coefficient values of the SVM models from all iterations in MVPA and LOOVC approach based on slope of the aperiodic component (B) and delta power (E) of the power spectrum. C and F show power spectrum densities for low (LH) and high (HH) hypnotic susceptible individuals at channel AF8 where we observed the largest averaged coefficient value for SVM models based on slope of aperiodic component for the pre-induction period, and at channel Fz where we observed the lowest averaged coefficient value for SVM models based on the delta power for Δ induction. Dotted lines show averaged aperiodic fit across participants for each spectrum. Full lines show averaged spectra.

For Δinduction, we observed altered delta power (**Figure 2D;** AUC = .57, $p < .01$). The corresponding topography highlights the frontal channels (**Figure 2E and 2F**). Examining the power values for channels where we examined the top 5% SVM weights (FP2, FP1, AF7), HHSIs appear to show greater delta power value during pre-induction period (**supplementary Figure 1D**). Note, however, that this difference is not captured by our multivariate approach. In turn, during the post-induction, HHSIs and LHSIs exhibit similar delta power values (**supplementary Figure 1E**). This pattern is consistent with our multivariate approach where we observed important changes between pre- and post-induction periods for HHSIs and relatively smaller changes for LHSIs (**supplementary Figure 1F**). Hence, after controlling for the aperiodic component of the PSD, our findings

reveal that the induction has a greater impact on delta band activity for HHSIs compared to LHSIs.

Network topology. For our graph theoretical approach, we first examined clustering coefficient. In the pre-induction rs-EEG recording, we found that the classification performance was statistically significant for clustering coefficient in the delta frequencies (**Figure 3A**; AUC value = .61, $p < .001$). Analyzing the weights of the classifiers, we observed widespread higher clustering coefficients in high hypnotic susceptible individuals, slightly concentrated in the central and bilateral temporal regions (**Figure 3B**). Furthermore, examining clustering coefficients for delta-band activity for channels where we observed the top 5% SVM weights indicate slightly higher coefficient values for HHSIs during the pre-induction period (CP6, TP9, C1, **supplementary Figure 2A**). No other classification patterns reached statistical significance for the pre-induction rs-EEG data (**Figure 3A**). These findings therefore provide further evidence of distinct neural characteristics associated with hypnotic susceptibility in the pre-induction state.

For Δinduction, we found that the classification performance was statistically significant in the alpha and beta frequency ranges (**Figure 3D**; AUC value for alpha-band activity = .55, $p < .05$; AUC value for beta-band activity = .59, $p < .001$). We observed opposite patterns between alpha-band and beta-band clustering coefficients, wherein HHSIs showed more pronounced decrease for the former and increase for the latter following the induction procedure (**Figure 3E** and **3G**; **supplementary Figure 2**). These findings provide evidence that the induction process yields greater changes in clustering coefficients for individuals with high hypnotic susceptibility compared to those with low hypnotic susceptibility.

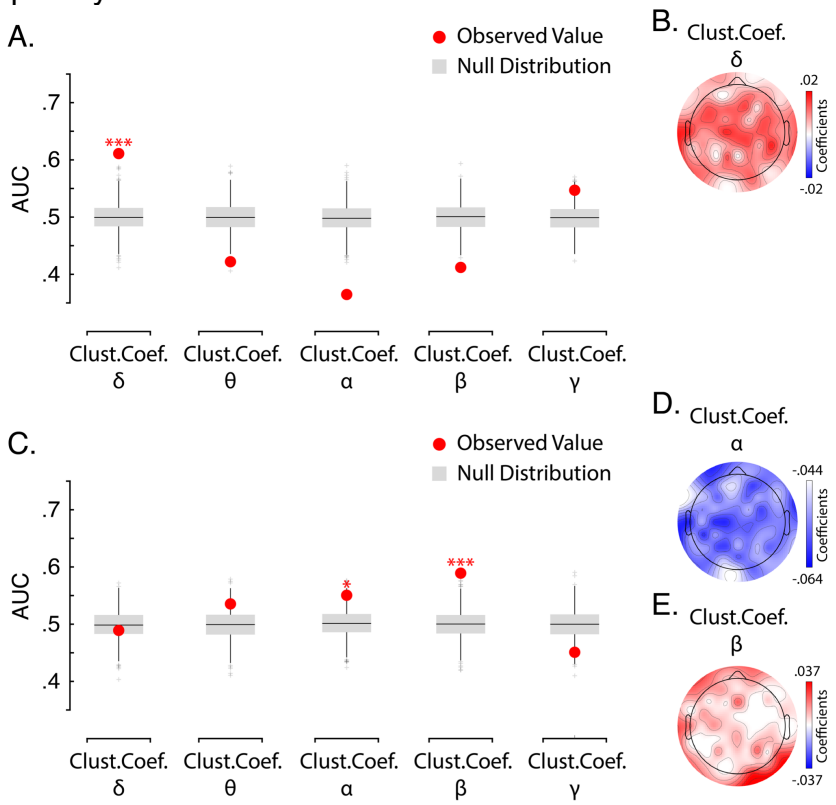

Figure 3. Panels A and D show AUC values for assessing classification performances of SVM linear models for accurately classifying high and low hypnotic susceptible individuals using LOOVC based on graph theory clustering coefficient calculated from pairwise wPLI across frequency bands during the rs-EEG pre-induction period (A) and for Δinduction (D). Red dots show observed AUC values. Boxplot shows surrogate null distributions based on random permutations where we shuffled the labels during training. One asterisk indicates statistical significance at $p < .05$, and three asterisks at $p < .001$. Panels B, E and G show the averaged coefficient values of the SVM models from all iterations during our multivariate classification and LOOVC approach based on clustering coefficients in the delta frequencies for the pre-induction rs-EEG period (B), as well as alpha (E) and beta (G) frequencies for Δinduction. Panels C, F and H show normalized wPLI values for low (LH) and high (HH) hypnotic susceptible individuals in the delta frequency band for the pre-induction procedure (C), as well as for Δinduction in the alpha (F) and beta (H) frequencies. Red lines indicate positive values and blue lines negative ones.

Next, we used logistic regression analyses to examine the effects of hypnotic susceptibility and the induction procedure on global efficiency and modularity at the network level. For the pre-induction rs-EEG data, the logistic regression model (VIFs < 2.8) indicates that global efficiency in delta band activity was a statistically reliable predictor of hypnotic susceptibility (**Figure 4A**). Here, greater global efficiency predicts high hypnotic susceptibility during the pre-induction rs-EEG period (β = 20.16, 95% C.I. [1.3, 39.02]; **Figure 4B**). For Δinduction, the logistic regression model (VIFs < 2.5) revealed that global efficiency in the theta frequencies (β = 18.9, 95% C.I. [.92, 36.99]) and modularity in the delta frequencies (β = -126.01, 95% C.I. [-246.67, -5.35]) were statistically significant predictors (**Figure 4C**). Specifically, the induction procedure was associated with increased global efficiency in the theta frequencies (**Figure 4D**) and decreased modularity (**Figure 4E**) in the delta frequencies in individuals with high hypnotic susceptibility compared to those with low hypnotic susceptibility.

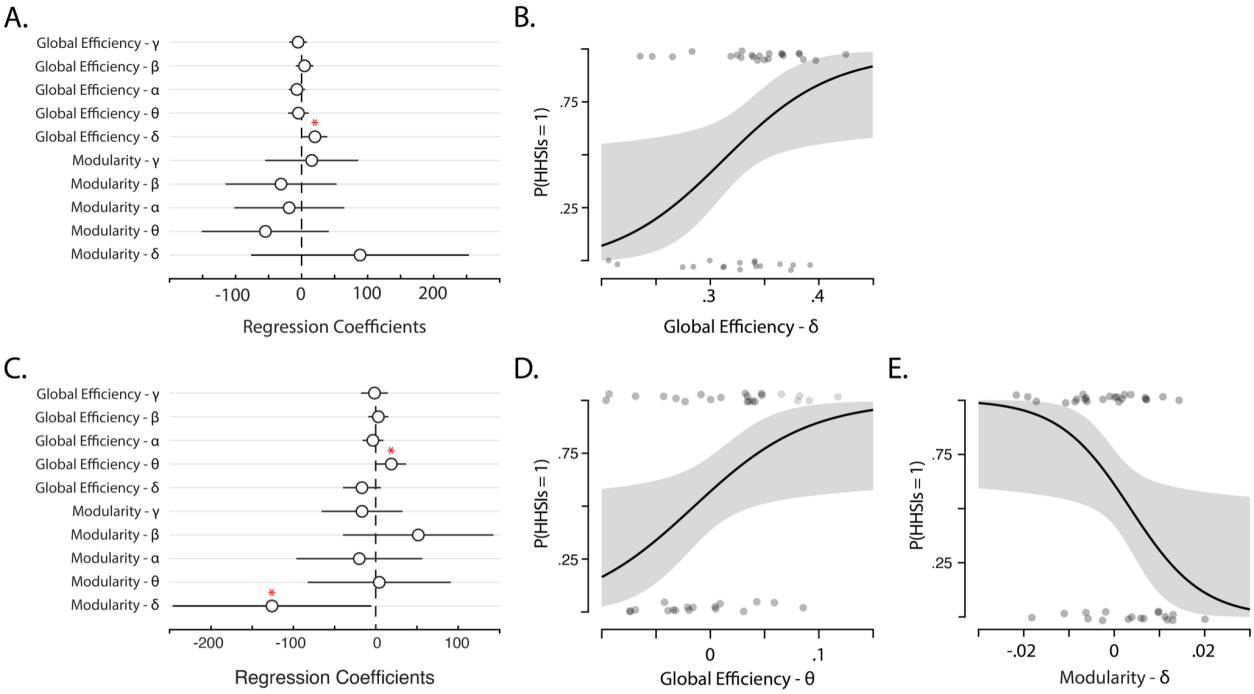

Figure 4. Panel **A** shows the coefficient values and 95 C.I. for our logistic regression model assessing if global efficiency and modularity for pre-induction rs-EEG across all frequency bands predict hypnotic

susceptibility. Panels **B** show likelihood estimates for significant coefficients, global efficiency in the delta frequency band. Each dot represents individual data points and grey area represents 95% C.I. Panel **C** shows the coefficient values and 95 C.I. for our logistic regression model assessing if global efficiency and modularity for Δinduction across all frequency bands predict hypnotic susceptibility. Panels **D** and **E** show likelihood estimates for significant coefficients, global efficiency in the theta frequency band and modularity in the theta frequency band, respectively. Each dot represents individual data points and grey area represents 95% C.I. Red asterisks indicate significant coefficient at $p < .05$.

Model comparisons. We used model comparisons to identify the most dominating feature among those we previously identified as statistically significant. Our approach involved systematically evaluating all combinations of statistically significant spectral features and graph theory metrics and then assessing the classification performance of these models. This analysis was first performed separately for the pre-induction rs-EEG period and the effect of the induction procedure (post minus pre-induction) rs-EEG period. We then compared the performance of all models in a pairwise manner using the McNemar test and corrected the p-values for multiple comparisons using the false discovery rate (FDR) method. This approach allowed us to assess which combination of variables provided the best classification performance for each period.

In our analysis of the pre-induction period, we previously identified the exponent of the aperiodic component, clustering coefficient and global efficiency in delta band activity as reliable EEG variables for classifying hypnotic susceptibility (**Figure 5A**). Combinations of these features yielded 7 models overall. Our results show that the models incorporating the slope of the aperiodic component consistently outperformed the other models, as indicated by higher AUC values for all these models (**Figure 5A**). The McNemar's Chi-square statistics confirmed the advantage of these models over classification performance (**Figure 5B**). Comparing models that include clustering coefficient and global efficiency in the delta range with versus without the aperiodic slope significantly alters classification performance.

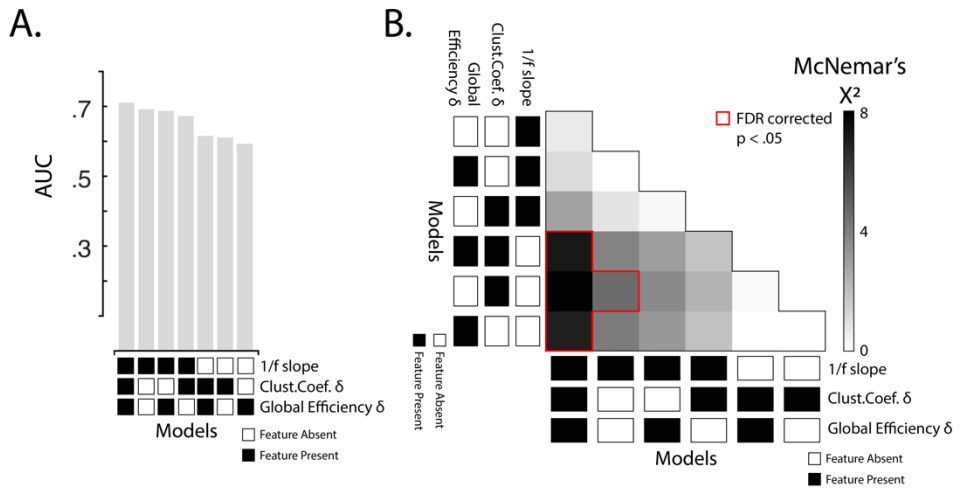

Figure 5. Panel A shows the AUC values for each model that were evaluated for the discrimination of high versus low hypnotic susceptible individuals based on the pre-induction rs-EEG. All three features had been identified via previous analyses. The x-axis shows the neural features that were included in each model whereby a full square indicates that the neural feature was included in the model, whereas an empty one

indicates that the feature was not included in the model. Panel B shows the corresponding McNemar's Chi-square statistics where we compared all models in a pairwise manner. Red contours indicate statistically significant comparisons after FDR corrections for multiple comparisons.

We applied the same model comparisons approach for Δinduction. These variables included changes in delta power, clustering coefficient in delta and beta ranges, global efficiency in the theta band, and modularity in the delta frequency band. All combinations of these features yielded a total of 31 models. Among these models, four models encompassing modularity in delta range achieved the highest classification scores (**Figure 6A**). The results of McNemar's Chi-square statistics supported these findings, demonstrating that these four models outperformed the other ones (**Figure 6B**).

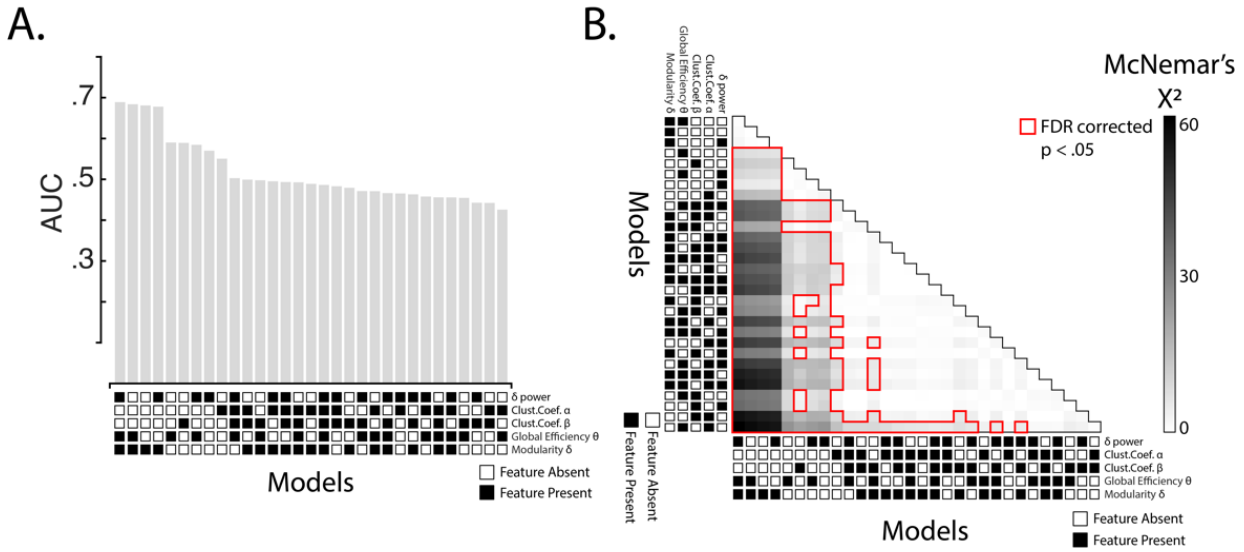

Figure 6. Panel A shows the AUC values for each model that were evaluated for the discrimination of high versus low hypnotic susceptible individuals based on neural features from the rs-EEG for the effect of the induction (post minus pre-induction) over rs-EEG. All five features had been identified via previous analyses. The x-axis shows the neural features that were included in each model whereby a full square indicates that the neural feature was included in the model, whereas an empty one indicates that the feature was not included in the model. Panel B shows the corresponding McNemar's Chi-square statistics where we compared all models in a pairwise manner. Red contours indicate statistically significant comparisons after FDR corrections for multiple comparisons.

We further compared all models encompassing features from both the pre-induction rs-EEG and Δinduction (**Figure 7A**). This final comparison highlights that the top models involve the slope of the aperiodic component, as evidenced by McNemar's chi-square statistics (**Figure 7B**).

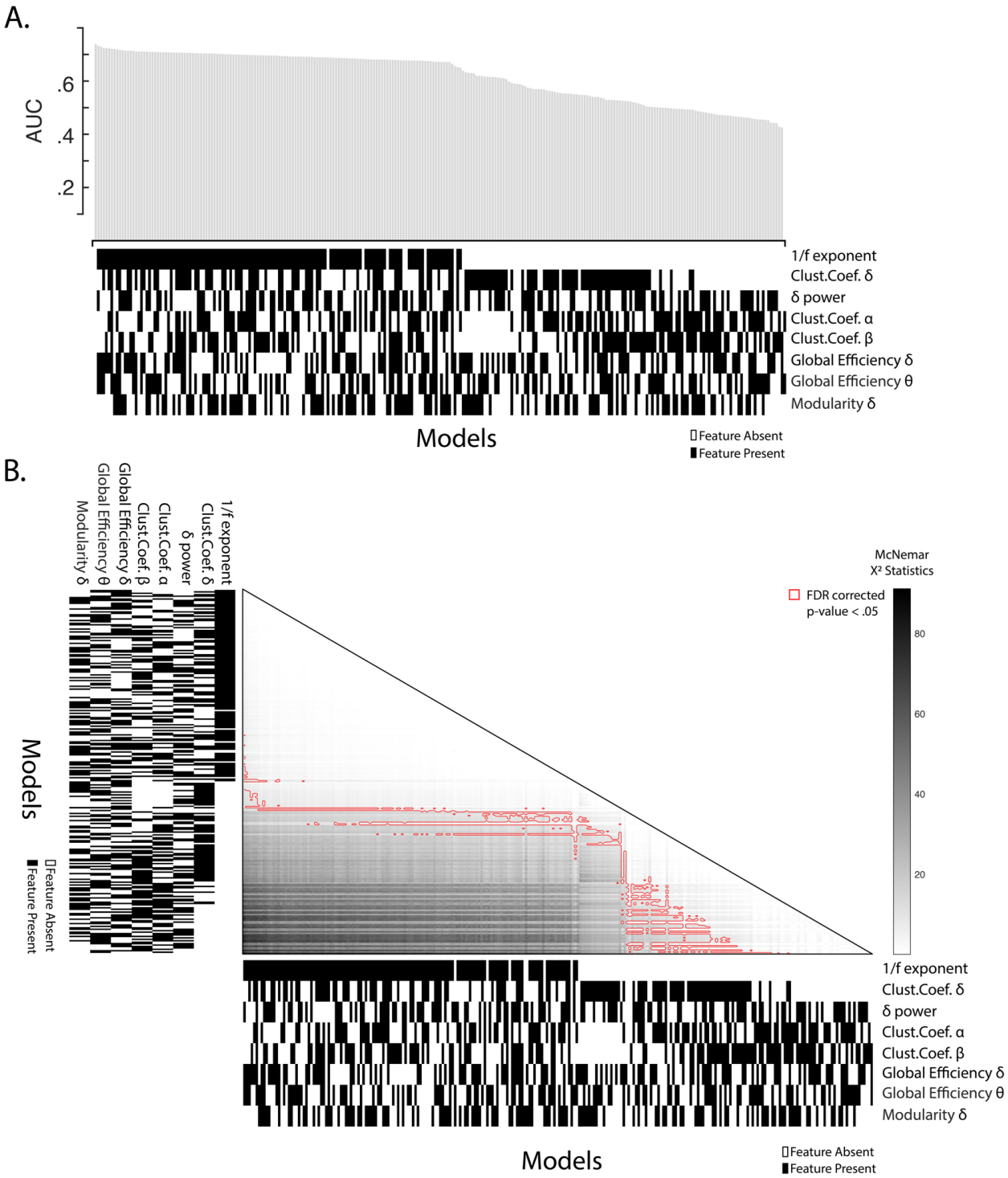

Figure 7. Panel A shows AUC values for each model that were evaluated for the discrimination of high versus low hypnotic susceptible individuals based on neural features from rs-EEG from the pre-induction period and Δinduction. All features had been identified via previous analyses. The x-axis shows the neural features that were included in each model whereby a black square indicates that the neural feature was included in the model, whereas a white square indicates that the feature was not included in the model. Panel B shows the corresponding McNemar's Chi-square statistics where we compared all models in a pairwise manner. Red contours indicate statistically significant comparisons after FDR corrections for multiple comparisons.

Neural feature ranking. Beyond comparisons of models, we sought to rank the pertinent neural features by their SVM weights based on the SVM model incorporating all relevant features. Examining feature ranking for the pre-induction period, the SVM model discriminated hypnotic susceptibility better than chance-level (AUC value = .61, $p < .001$). For this model, the exponent of the aperiodic component emerged as the most discriminative feature (**Figure 8A**). In turn, when we evaluated all significant features related to the effect of the induction procedure (post- minus pre-induction) together, the model's performance was not better than chance-level. Lastly, when we included all significant features from both the pre-induction period and from the effect of the induction procedure, the model did perform above chance-level (AUC value = .69, $p < .001$). Again, the exponent of aperiodic component for the pre-induction resting-state period was the most discriminant feature, followed by the clustering coefficient of alpha-band activity in rs-EEG pertaining to the effect of the induction procedure (**Figure 8B**). Collectively, these analyses highlight the centrality of aperiodic EEG activity for discriminating hypnotic susceptibility.

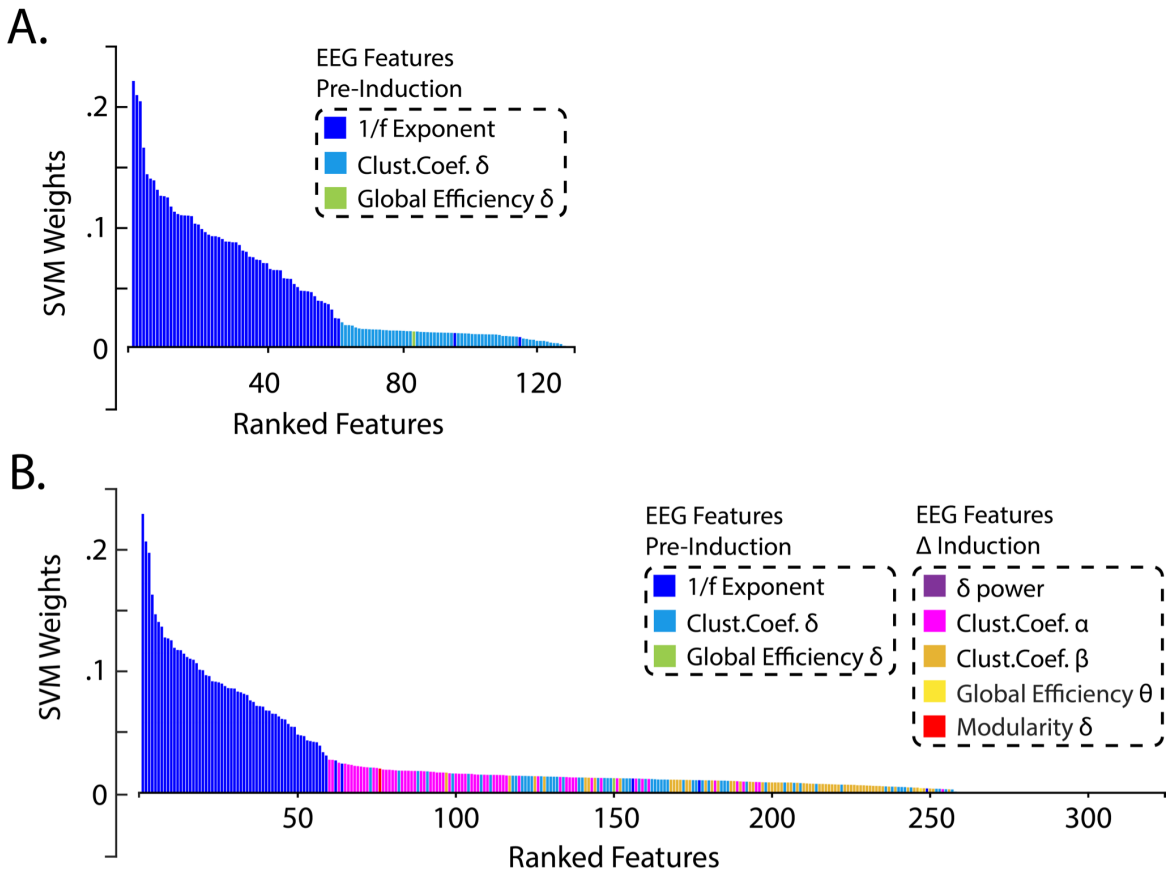

Figure 8. Weights of SVM classifiers trained to differentiate high and low hypnotic susceptibility using rs-EEG features. Panel A: Features from the pre-induction period. Panel B Δinduction. Features were identified in preceding analyses. The x-axis ranks neural features in descending order, while the y-axis displays the absolute values of the SVM weights.

Discussion

The current study provides a comprehensive investigation into the neural features that underlie both hypnotic susceptibility and the hypnotic induction process – two pivotal variables of hypnotic phenomena. We analyzed various neural features, which encompass power spectra and connectivity patterns, from rs-EEG recordings taken pre- and post-hypnotic induction. Employing a combination of multivariate pattern classification and LOOCV, our results support the notion that hypnosis possesses multiple dimensions and correlates with diverse neural attributes. In the rs-EEG taken before the induction, our classifiers distinguished between individuals with high and low hypnotic susceptibility better than random predictions across several neural features. These features included the aperiodic exponent of the power spectrum (**Figure 2**), and the clustering coefficient (**Figure 3**) and global efficiency (**Figure 4**) in the delta frequency range. These findings highlight the neural features that set apart individuals based on their hypnotic susceptibility, corroborating earlier functional neuroimaging studies (Hoeft et al., 2012; Huber et al., 2014). Susceptibility to hypnotic suggestion therefore reflects a predisposition that is captured by neural features independent from the hypnotic procedure. However, note that participants were not blind to the context of this experiment, which entails that findings regarding the pre-induction period likely include effects of expectations (Coe & Sarbin, 1977; Gandhi & Oakley, 2005).

From the rs-EEG pertaining to the effects of the induction (i.e., Δinduction), the classifiers showcased performances surpassing chance levels in detecting variations for delta power (**Figure 2**), clustering coefficients across alpha and beta bands (**Figure 3**), and both global efficiency in the theta band and global modularity in the delta band (**Figure 4**). Importantly, our results reveal the influence of the induction procedure on delta-band activity after controlling for the aperiodic component for the EEG signal. Furthermore, these results highlight the influence of the induction process on diverse aspects of brain dynamics relative to susceptibility to hypnotic suggestion, which aligns with recent work (Panda et al., 2023). This observation reinforces the idea that the induction process shifts both spectral power and network topology across various frequency bands. Indeed, Panda and colleagues highlighted changes in connectivity patterns throughout delta, alpha, and beta frequencies due to the induction process. The induction procedure relates to increased mental absorption, feelings of relaxation, and preparation for hypnotic responding (Terhune & Cardeña, 2016). The effects observed relative to network topologies are likely indicative of the differential expression of these mental states between highly and less hypnotizable subjects. Interestingly, analogous shifts in network structures across delta, alpha, and beta frequencies have been observed when comparing neural patterns of novice and expert meditators (Lardone et al., 2022; van Lutterveld et al., 2017). This observation resonates with the hypothesis suggesting a convergence between hypnosis and meditative practices (Raz & Lifshitz, 2016). Both practices encompass the involvement of attention resources and the recruitment of the same brain networks (Landry & Raz, 2016; Lifshitz et al., 2019).

Importantly, we employed model comparisons and feature ranking to discern the most salient neural features that differentiate between high and low hypnotic susceptibility across pre- and post-induction periods. Our data-driven methodologies reveal that the slope of the aperiodic component during the pre-induction period stands out as the

primary neural feature (**Figures 5, 7, and 8**). Notably, individuals with HHSIS exhibited a steeper slope compared to those with low hypnotic susceptibility LHSIS (**supplementary Figure 1A**). Our results echoes the importance of considering the aperiodic component of the power spectrum when examining the effects oscillatory activity (Donoghue et al., 2022), including neuroscientific research of hypnotic phenomena. Furthermore, the aperiodic component represents an alternative feature Moreover, previous EEG research might have led one to anticipate that the neural patterns emerging post-induction would be the principal distinguishing features (e.g., Terhune et al., 2011). This expectation is reinforced by prior work reporting modifications in long-range temporal correlations— a scale-free quantitative assessment of amplitude fluctuations in the signal that relates to the aperiodic component of the EEG —in response to hypnotic induction (Lee et al., 2007). Contrary to these expectations, we found that characteristics that separate HHSIs and LHSIs are already present in the pre-induction phase. This outcome supports the idea that hypnotic susceptibility reflects a cerebral predisposition and brings about the possibility of assessing it using rs-EEG at baseline instead of standardized protocols (Baghdadi & Nasrabadi, 2012). In this regards, mounting evidence proposes that ability for hypnotic responding is best captured by interrelated components characterized by a structure comprising a core ability that superordinate secondary ones (Barnier et al., 2022). One may conjecture that the centrality of the aperiodic slope for differentiating HHISs and LHSIs during the pre-induction period reflects this core component.

Furthermore, the anterior topographical pattern corresponding to this neural feature (**Figure 2B**) aligns with research positing that this predisposition for efficient hypnotic response is related with prefrontal cortex (PFC) activity (Cojan et al., 2015; Hoeft et al., 2012). Several studies have connected these patterns of PFC activity in hypnotic susceptibility to fluctuations in executive functions (Egner & Raz, 2007; Faerman & Spiegel, 2021; Parris, 2017). In turn, greater cognitive control seemingly underlies phenomenological control – i.e., the inherent ability of controlling one's own subjective experiences as a function of expectancies and suggestions (Dienes & Lush, 2023; Lush et al., in press). However, links between the aperiodic component in EEG readings and executive functions remain largely tenuous and exploratory. While research on the aperiodic component is nascent (Donoghue et al., 2022), emerging evidence reveals that cognitive impairments, including shifts in executive functioning, are associated with a less pronounced slope in the aperiodic component (Finley et al., 2023). Moreover, prevailing accounts propose that the slope of the aperiodic exponent corresponds to the balance between excitatory and inhibitory activities of neural populations (Gao et al., 2017; Waschke et al., 2021). In this framework, lower slope values indicate unbalanced activity and increased noise during information processing, thereby leading to poorer cognitive performance (Voytek & Knight, 2015). Greater slope values in HHSIs relative to LHSIs could therefore account for different executive control and cognitive control abilities. Nevertheless, additional research specifically examining the relationship between hypnotic susceptibility differences, executive functions and the aperiodic component is paramount before any definitive conclusions can be drawn.

In summary, our study contributes to the expanding literature that underscores the significance of the aperiodic component in rs-EEG signals in elucidating inter-individual

neural variations (Bódizs et al., 2021; Cellier et al., 2021; Immink et al., 2021; Schaworonkow & Voytek, 2021; Waschke et al., 2017). Through a data-driven methodology, we identified distinct neural features across the power spectrum and graph theory both pre- and post-hypnotic induction, enhancing our ability to discriminate between HHSIs and LHSIs beyond chance levels. Instead of pinpointing a singular neural pattern, our results corroborate the understanding that hypnotic experiences possess a layered neural foundation (Landry & Rainville, in press). A surprising finding was the prominence of the slope of aperiodic EEG activity in the pre-induction phase as the key neural feature. This outcome promotes the idea that baseline brain activity offers a more accurate representation of hypnotic susceptibility than the effects stemming from the induction process itself. Our observations underscore the value of focusing on this aspect of the power spectrum in future explorations of the neural underpinnings of hypnotic experiences. Furthermore, this finding resonates with the hypothesis that hypnotic susceptibility is an inherent psychological trait predisposing certain individuals to be more responsive to suggestions. Collectively, our research illuminates the intricate neural dynamics surrounding hypnotic experiences, highlighting varied neural markers linked to hypnotic susceptibility both prior to and following induction.

References

Baghdadi, G., & Nasrabadi, A. M. (2012). Comparison of different EEG features in estimation of hypnosis susceptibility level. *Computers in biology and medicine, 42*(5), 590-597.

Barnier, A. J., Cox, R. E., & McConkey, K. M. (2014). The Province of "Highs": The High Hypnotizable Person in the Science of Hypnosis and in Psychological Science. *Psychology of Consciousness: Theory, Research, and Practice, 1*(2), 168-183.

Barnier, A. J., Terhune, D. B., Polito, V., & Woody, E. Z. (2022). A componential approach to individual differences in hypnotizability. *Psychology of Consciousness: Theory, Research, and Practice, 9*(2), 130.

Bódizs, R., Szalárdy, O., Horváth, C., Ujma, P. P., Gombos, F., Simor, P., Pótári, A., Zeising, M., Steiger, A., & Dresler, M. (2021). A set of composite, non-redundant EEG measures of NREM sleep based on the power law scaling of the Fourier spectrum. *Scientific Reports, 11*(1), 2041.

Braffman, W., & Kirsch, I. (1999, Sep). Imaginative suggestibility and hypnotizability: an empirical analysis. *J Pers Soc Psychol, 77*(3), 578-587.

Bullmore, E., & Sporns, O. (2009). Complex brain networks: graph theoretical analysis of structural and functional systems. *Nature Reviews Neuroscience, 10*(3), 186-198.

Buzsáki, G., & Draguhn, A. (2004). Neuronal oscillations in cortical networks. *Science, 304*(5679), 1926-1929.

Cardeña, E. (2005). The phenomenology of deep hypnosis: Quiescent and physically active. *International Journal of Clinical and Experimental Hypnosis, 53*(1), 37-59.

Cardeña, E. (2014). Hypnos and psyche: How hypnosis has contributed to the study of consciousness. *Psychology of Consciousness: Theory, Research, and Practice, 1*(2), 123.

Cardeña, E. (2016). Toward comprehensive neurophenomenological research in hypnosis and meditation. In *Hypnosis and meditation: Towards an integrative science of conscious planes.* (pp. 281-301). Oxford University Press.

Cellier, D., Riddle, J., Petersen, I., & Hwang, K. (2021, 2021/08/01/). The development of theta and alpha neural oscillations from ages 3 to 24 years. *Developmental cognitive neuroscience, 50*, 100969.

Coe, W. C., & Sarbin, T. R. (1977, 1977/10/01). HYPNOSIS FROM THE STANDPOINT OF A CONTEXTUALIST. *Annals of the New York Academy of Sciences, 296*(1), 2-13.

Cohen, J. R., & D'Esposito, M. (2016, Nov 30). The Segregation and Integration of Distinct Brain Networks and Their Relationship to Cognition. *J Neurosci, 36*(48), 12083-12094.

Cole, M. W., Bassett, D. S., Power, J. D., Braver, T. S., & Petersen, S. E. (2014). Intrinsic and task-evoked network architectures of the human brain. *Neuron, 83*(1), 238-251.

Combrisson, E., & Jerbi, K. (2015, 2015/07/30/). Exceeding chance level by chance: The caveat of theoretical chance levels in brain signal classification and statistical assessment of decoding accuracy. *Journal of Neuroscience Methods, 250*, 126-136.

De Pascalis, V. (1993). EEG spectral analysis during hypnotic induction, hypnotic dream and age regression. *International journal of psychophysiology, 15*(2), 153-166.

Deeley, Q., Oakley, D. A., Toone, B., Giampietro, V., Brammer, M. J., Williams, S. C. R., & Halligan, P. W. (2012). Modulating the Default Mode Network Using Hypnosis. *International Journal of Clinical and Experimental Hypnosis, 60*(2), 206-228.

Demertzi, A., Soddu, A., Faymonville, M.-E., Bahri, M. A., Gosseries, O., Vanhaudenhuyse, A., Phillips, C., Maquet, P., Noirhomme, Q., Luxen, A., & Laureys, S. (2011). Hypnotic modulation of resting state fMRI default mode and extrinsic network connectivity. *Progress in Brain Research, 193*, 309-322.

Desmarteaux, C., Streff, A., Chen, J.-I., Houzé, B., Piché, M., & Rainville, P. (2021). Brain responses to hypnotic verbal suggestions predict pain modulation. *Frontiers in Pain Research, 2*, 757384.

Dienes, Z., & Lush, P. (2023, 2023/04/01). The Role of Phenomenological Control in Experience. *Current directions in psychological science, 32*(2), 145-151.

Dienes, Z., & Perner, J. (2007). Executive control without conscious awareness: the cold control theory. In G. A. Jamieson (Ed.), *Hypnosis and conscious states: The cognitive neuroscience perspective* (pp. 293-314). Oxford University Press.

Dietterich, T. G. (1998). Approximate statistical tests for comparing supervised classification learning algorithms. *Neural computation, 10*(7), 1895-1923.

Donoghue, T., Haller, M., Peterson, E. J., Varma, P., Sebastian, P., Gao, R., Noto, T., Lara, A. H., Wallis, J. D., Knight, R. T., Shestyuk, A., & Voytek, B. (2020, 2020/12/01). Parameterizing neural power spectra into periodic and aperiodic components. *Nature neuroscience, 23*(12), 1655-1665.

Donoghue, T., Schaworonkow, N., & Voytek, B. (2022, 2022/06/01). Methodological considerations for studying neural oscillations. *European Journal of Neuroscience, 55*(11-12), 3502-3527.

Egner, T., & Raz, A. (2007). Cognitive Control Processes and Hypnosis. In G. A. Jamieson (Ed.), *Hypnosis and Conscious States: The cognitive neuroscience perspective* (pp. 29-50). Oxford University Press.

Elkins, G. (2016). *Clinician's Guide to Medical and Psychological Hypnosis: Foundations, Applications, and Professional Issues*. Springer Publishing Company.

Faerman, A., & Spiegel, D. (2021). Shared cognitive mechanisms of hypnotizability with executive functioning and information salience. *Scientific Reports, 11*(1), 5704.

Farahani, F. V., Karwowski, W., & Lighthall, N. R. (2019). Application of graph theory for identifying connectivity patterns in human brain networks: a systematic review. *frontiers in Neuroscience, 13*, 585.

Finley, A. J., Angus, D. J., Knight, E., van Reekum, C. M., Lachman, M. E., Davidson, R. J., & Schaefer, S. M. (2023). Resting EEG Periodic and Aperiodic Components Predict Cognitive Decline Over 10 Years. *bioRxiv*, 2023-2007.

Gandhi, B., & Oakley, D. A. (2005). Does 'hypnosis' by any other name smell as sweet? The efficacy of 'hypnotic'inductions depends on the label 'hypnosis'. *Consciousness and cognition, 14*(2), 304-315.

Gao, R., Peterson, E. J., & Voytek, B. (2017). Inferring synaptic excitation/inhibition balance from field potentials. *NeuroImage, 158*, 70-78.

Gerster, M., Waterstraat, G., Litvak, V., Lehnertz, K., Schnitzler, A., Florin, E., Curio, G., & Nikulin, V. (2022). Separating neural oscillations from aperiodic 1/f activity: challenges and recommendations. *Neuroinformatics*, 1-22.

Haufe, S., Meinecke, F., Görgen, K., Dähne, S., Haynes, J.-D., Blankertz, B., & Bießmann, F. (2014). On the interpretation of weight vectors of linear models in multivariate neuroimaging. *NeuroImage, 87*, 96-110.

He, B. J. (2014, 2014/09/01/). Scale-free brain activity: past, present, and future. *Trends in cognitive sciences, 18*(9), 480-487.

Hoeft, F., Gabrieli, J. D., Whitfield-Gabrieli, S., Haas, B. W., Bammer, R., Menon, V., & Spiegel, D. (2012). Functional brain basis of hypnotizability. *Archives of General Psychiatry, 69*(10), 1064-1072.

Huber, A., Lui, F., Duzzi, D., Pagnoni, G., & Porro, C. A. (2014). Structural and Functional Cerebral Correlates of Hypnotic Suggestibility. *PloS one, 9*(3), e93187.

Immink, M. A., Cross, Z. R., Chatburn, A., Baumeister, J., Schlesewsky, M., & Bornkessel-Schlesewsky, I. (2021). Resting-state aperiodic neural dynamics predict individual differences in visuomotor performance and learning. *Human Movement Science, 78*, 102829.

Jamieson, G. A., & Burgess, A. P. (2014). Hypnotic induction is followed by state-like changes in the organization of EEG functional connectivity in the theta and beta frequency bands in high-hypnotically susceptible individuals. *Frontiers in human neuroscience, 8*, 528.

JASP Team (2023). *JASP*

Jiang, H., White, M. P., Greicius, M. D., Waelde, L. C., & Spiegel, D. (2016). Brain Activity and Functional Connectivity Associated with Hypnosis. *Cerebral Cortex, 27*(8), 4083-4093.

Keshmiri, S., Alimardani, M., Shiomi, M., Sumioka, H., Ishiguro, H., & Hiraki, K. (2020). Higher hypnotic suggestibility is associated with the lower EEG signal variability in theta, alpha, and beta frequency bands. *PloS one, 15*(4), e0230853.

Kirsch, I., & Braffman, W. (2001). Imaginative Suggestibility and Hypnotizability. *Current directions in psychological science, 10*(2), 57-61.

Landry, M., Lifshitz, M., & Raz, A. (2017, 2017/10/01/). Brain correlates of hypnosis: A systematic review and meta-analytic exploration. *Neuroscience & Biobehavioral Reviews, 81*, 75-98.

Landry, M., & Rainville, P. (in press). Beyond the neural signature of hypnosis: Neuroimaging studies support a multifaceted view of hypnotic phenomena. In J. Linden, L. Sugerman, G. de Benedittis, & K. Varga (Eds.), *Routledge International Handbook of Clinical Hypnosis*. Taylor & Francis.

Landry, M., & Raz, A. (2015). Hypnosis and imaging of the living brain. *American Journal of Clinical Hypnosis, 57*(3), 285-313.

Landry, M., & Raz, A. (2016). Heightened states of attention: From mental performance to altered states of consciousness and contemplative practices. *Intellectica, 66*, 139-159.

Lardone, A., Liparoti, M., Sorrentino, P., Minino, R., Polverino, A., Lopez, E. T., Bonavita, S., Lucidi, F., Sorrentino, G., & Mandolesi, L. (2022). Topological changes of brain network during mindfulness meditation: an exploratory source level magnetoencephalographic study. *AIMS Neuroscience, 9*(2), 250-263.

Latora, V., & Marchiori, M. (2001, 10/17/). Efficient Behavior of Small-World Networks. *Physical Review Letters, 87*(19), 198701.

Laurence, J.-R., Beaulieu-Prévost, D., & Du Chéné, T. (2008). Measuring and understanding individual differences in hypnotizability. In A. J. Barnier & M. R. Nash (Eds.), *The Oxford Handbook of Hypnosis: Theory, Research, and Practice*. Oxford University Press.

Lee, J.-S., Spiegel, D., Kim, S.-B., Lee, J.-H., Kim, S.-I., Yang, B.-H., Choi, J.-H., Kho, Y.-C., & Nam, J.-H. (2007). Fractal analysis of EEG in hypnosis and its relationship with hypnotizability. *Intl. Journal of Clinical and Experimental Hypnosis, 55*(1), 14-31.

Lifshitz, M., van Elk, M., & Luhrmann, T. M. (2019, 2019/08/01/). Absorption and spiritual experience: A review of evidence and potential mechanisms. *Consciousness and cognition, 73*, 102760.

Lopes da Silva, F. (2013, 2013/12/04/). EEG and MEG: Relevance to Neuroscience. *Neuron, 80*(5), 1112-1128.

Lush, P., Dienes, Z., & Seth, A. (in press). Expectancies and the generation of perceptual experience: Predictive processing and phenomenological control. In T. Cheng, R. Sato, & H. Jacob (Eds.), *Expected Experiences: The predictive mind in an uncertain world*. Routledge.

Lynn, S. J., Green, J. P., Polizzi, C. P., Ellenberg, S., Gautam, A., & Aksen, D. (2019, 2019/10/02). Hypnosis, Hypnotic Phenomena, and Hypnotic Responsiveness: Clinical and Research Foundations—A 40-Year Perspective. *International Journal of Clinical and Experimental Hypnosis, 67*(4), 475-511.

Maschke, C., Duclos, C., Owen, A. M., Jerbi, K., & Blain-Moraes, S. (2023, 2023/07/15/). Aperiodic brain activity and response to anesthesia vary in disorders of consciousness. *NeuroImage, 275*, 120154.

Mazzoni, G., Venneri, A., McGeown, W. J., & Kirsch, I. (2013). Neuroimaging resolution of the altered state hypothesis. *Cortex, 49*(2), 400-410.

McGeown, W. J., Mazzoni, G., Venneri, A., & Kirsch, I. (2009). Hypnotic induction decreases anterior default mode activity. *Consciousness and cognition, 18*(4), 848-855.

McNemar, Q. (1947). Note on the sampling error of the difference between correlated proportions or percentages. *Psychometrika, 12*(2), 153-157.

Miller, K. J., Sorensen, L. B., Ojemann, J. G., & Den Nijs, M. (2009). Power-law scaling in the brain surface electric potential. *PLoS computational biology, 5*(12), e1000609.

Montgomery, G. H., Schnur, J. B., & David, D. (2011). The impact of hypnotic suggestibility in clinical care settings. *International Journal of Clinical and Experimental Hypnosis, 59*(3), 294-309.

Nash, M. R., & Barnier, A. J. (2008). *The Oxford handbook of hypnosis : theory, research and practice*. Oxford University Press.

Newman, M. E. (2006). Modularity and community structure in networks. *Proceedings of the national academy of sciences, 103*(23), 8577-8582.

Onnela, J.-P., Saramäki, J., Kertész, J., & Kaski, K. (2005, 06/13/). Intensity and coherence of motifs in weighted complex networks. *Physical Review E, 71*(6), 065103.

Panda, R., Vanhaudenhuyse, A., Piarulli, A., Annen, J., Demertzi, A., Alnagger, N., Chennu, S., Laureys, S., Faymonville, M.-E., & Gosseries, O. (2023). Altered Brain Connectivity and Network Topological Organization in a Non-ordinary State of Consciousness Induced by Hypnosis. *Journal of Cognitive Neuroscience, 35*(9), 1394-1409.

Parris, B. A. (2017). The role of frontal executive functions in hypnosis and hypnotic suggestibility. *Psychology of Consciousness: Theory, Research, and Practice, 4*(2), 211-229.

Pekala, R. J. (2015). Hypnosis as a “state of consciousness”: How quantifying the mind can help us better understand hypnosis. *American Journal of Clinical Hypnosis, 57*(4), 402-424.

Pekala, R. J., & Kumar, V. K. (2007). An empirical—phenomenological approach to quantifying consciousness. In G. Jamieson (Ed.), *Hypnosis and conscious states: The cognitive neuroscience perspective* (pp. 167-194). Oxford University Press.

Rainville, P., Duncan, G. H., Price, D. D., Carrier, B., & Bushnell, M. C. (1997). Pain affect encoded in human anterior cingulate but not somatosensory cortex. *Science, 277*(5328), 968-971.

Rainville, P., Hofbauer, R. K., Paus, T., Duncan, G. H., Bushnell, M. C., & Price, D. D. (1999). Cerebral mechanisms of hypnotic induction and suggestion. *Journal of Cognitive Neuroscience, 11*(1), 110-125.

Rainville, P., & Price, D. D. (2003). Hypnosis phenomenology and the neurobiology of consciousness. *International Journal of Clinical and Experimental Hypnosis, 51*(2), 105-129.

Rainville, P., Streff, A., Chen, J.-I., Houzé, B., Desmarteaux, C., & Piché, M. (2019). Hypnotic automaticity in the brain at rest: An arterial spin labelling study. *International Journal of Clinical and Experimental Hypnosis, 67*(4), 512-542.

Raz, A., & Lifshitz, M. (2016). *Hypnosis and meditation: Towards an integrative science of conscious planes*. Oxford University Press.

Rubinov, M., & Sporns, O. (2010). Complex network measures of brain connectivity: uses and interpretations. *NeuroImage, 52*(3), 1059-1069.

Rubinov, M., & Sporns, O. (2011). Weight-conserving characterization of complex functional brain networks. *NeuroImage, 56*(4), 2068-2079.

Sabourin, M. E., Cutcomb, S. D., Crawford, H. J., & Pribram, K. (1990). EEG correlates of hypnotic susceptibility and hypnotic trance: Spectral analysis and coherence. *International journal of psychophysiology, 10*(2), 125-142.

Schaworonkow, N., & Voytek, B. (2021). Longitudinal changes in aperiodic and periodic activity in electrophysiological recordings in the first seven months of life. *Developmental cognitive neuroscience, 47*, 100895.

Shor, R. E., & Orne, E. C. (1962). *Harvard group scale of hypnotic susceptibility, Form: A*. Consulting psychologists press.

Spiegel, D., Cutcomb, S., Ren, C., & Pribram, K. (1985). Hypnotic hallucination alters evoked potentials. *Journal of Abnormal Psychology, 94*(3), 249.

Tadel, F., Baillet, S., Mosher, J. C., Pantazis, D., & Leahy, R. M. (2011). Brainstorm: a user-friendly application for MEG/EEG analysis. *Computational intelligence and neuroscience, 2011*, 8.

Terhune, D. B., & Cardeña, E. (2016). Nuances and Uncertainties Regarding Hypnotic Inductions: Toward a Theoretically Informed Praxis. *American Journal of Clinical Hypnosis, 59*(2), 155-174.

Terhune, D. B., Cardeña, E., & Lindgren, M. (2011). Differential frontal-parietal phase synchrony during hypnosis as a function of hypnotic suggestibility. *Psychophysiology, 48*(10), 1444-1447.

Terhune, D. B., Cleeremans, A., Raz, A., & Lynn, S. J. (2017). Hypnosis and top-down regulation of consciousness. *Neuroscience & Biobehavioral Reviews*.

Thölke, P., Mantilla-Ramos, Y.-J., Abdelhedi, H., Maschke, C., Dehgan, A., Harel, Y., Kemtur, A., Berrada, L. M., Sahraoui, M., & Young, T. (2022). Class imbalance should not throw you off balance: Choosing the right classifiers and performance metrics for brain decoding with imbalanced data. *bioRxiv*, 2022-2007.

Timmermann, C., Bauer, P. R., Gosseries, O., Vanhaudenhuyse, A., Vollenweider, F., Laureys, S., Singer, T., Antonova, E., & Lutz, A. (2023, 2023/02/01/). A neurophenomenological approach to non-ordinary states of consciousness: hypnosis, meditation, and psychedelics. *Trends in cognitive sciences, 27*(2), 139-159.

van Lutterveld, R., van Dellen, E., Pal, P., Yang, H., Stam, C. J., & Brewer, J. (2017, 2017/09/01/). Meditation is associated with increased brain network integration. *NeuroImage, 158*, 18-25.

Vanhaudenhuyse, A., Laureys, S., & Faymonville, M. E. (2014, 10//). Neurophysiology of hypnosis. *Neurophysiologie Clinique/Clinical Neurophysiology, 44*(4), 343-353.

Vanhaudenhuyse, A., Ledoux, D., Gosseries, O., Demertzi, A., Laureys, S., & Faymonville, M.-E. (2019). Can subjective ratings of absorption, dissociation, and time perception during “neutral hypnosis” predict hypnotizability?: An exploratory study. *International Journal of Clinical and Experimental Hypnosis, 67*(1), 28-38.

Vinck, M., Oostenveld, R., van Wingerden, M., Battaglia, F., & Pennartz, C. M. A. (2011). An improved index of phase-synchronization for electrophysiological data in the presence of volume-conduction, noise and sample-size bias. *NeuroImage, 55*(4), 1548-1565.

Voytek, B., & Knight, R. T. (2015). Dynamic network communication as a unifying neural basis for cognition, development, aging, and disease. *Biological psychiatry, 77*(12), 1089-1097.

Wang, R., Liu, M., Cheng, X., Wu, Y., Hildebrandt, A., & Zhou, C. (2021, 2021/06/08). Segregation, integration, and balance of large-scale resting brain networks configure different cognitive abilities. *Proceedings of the national academy of sciences, 118*(23), e2022288118.

Waschke, L., Donoghue, T., Fiedler, L., Smith, S., Garrett, D. D., Voytek, B., & Obleser, J. (2021). Modality-specific tracking of attention and sensory statistics in the human electrophysiological spectral exponent. *Elife, 10*, e70068.

Waschke, L., Wöstmann, M., & Obleser, J. (2017, 2017/12/12). States and traits of neural irregularity in the age-varying human brain. *Scientific Reports, 7*(1), 17381.

Weitzenhoffer, A. M. (1980). Hypnotic susceptibility revisited. *American Journal of Clinical Hypnosis, 22*(3), 130-146.

Wilson, L. E., da Silva Castanheira, J., & Baillet, S. (2022, 2022/09/12). Time-resolved parameterization of aperiodic and periodic brain activity. *Elife, 11*, e77348.

Woody, E. Z., & Barnier, A. J. (2008). Hypnosis scales for the twenty-first century: What do we need and how should we use them. *The Oxford handbook of hypnosis: Theory, research, and practice, Oxford University Press*, 255-282.

Woody, E. Z., Barnier, A. J., & McConkey, K. M. (2005). Multiple hypnotizabilities: differentiating the building blocks of hypnotic response. *Psychological assessment, 17*(2), 200.

Yapko, M. D. (2015). *Essentials of hypnosis* (2nd ed.). Routledge.